Proceedings of the 2007 IEEE
International Conference on Robotics and Biomimetics
December 15 -18, 2007, Sanya, China

# Towards a Mobile Airbag System Using MEMS Sensors and Embedded Intelligence

Guangyi Shi,[1] Cheung-Shing Chan,[3] Guanglie Zhang,[1] Wen J. Li,[1,*] Philip H. W. Leong[2] and Kwok-Sui Leung[3]

[1]Centre for Micro and Nano Systems    [2]Dept. of Computer Science and Eng.    [3]Dept. of Orthop. and Traum.

Faculty of Engineering      Faculty of Engineering      Faculty of Medicine

The Chinese University of Hong Kong

*Contact Author: wen@mae.cuhk.edu.hk

***Abstract*. This paper introduces the development of a mobile human airbag system designed for fall protection for the elderly. A Micro Inertial Measurement Unit (μIMU) that is 66 mm x 20 mm x 20 mm in size is built. This unit consists of three dimensional MEMS accelerometers, gyroscopes, MCU, and a Bluetooth module. It records human motion information, and, with a Support Vector Machine (SVM) training process, it can be used to classify falls and other normal motions successfully with an SVM filter. Based on the SVM filter, an embedded DSP (Digital Signal Processing) system is developed for real-time fall detection. Also, a smart mechanical airbag deployment system is finalized. This system weighs 253.5 grams (including a 42.5 g compressed $CO_2$ cylinder) with dimensions of 190 mm length, 57 mm width and 30 mm height. The response time of the mechanical trigger is 0.133 seconds, which has been proven in our lab to allow enough time for compressed air release before a person falls down to the ground. The integrated system is tested, and the feasibility of the airbag system for real-time fall protection is demonstrated.**

***Keywords: MEMS, μIMU, Human Motion Sensing, SVM, Mobile Airbags, DSP.***

## I   INTRODUCTION

The world is faced with an increasingly aging population. With this increase, the proportion of the elderly who are frail and dependent is also likely to increase significantly [1]. This shift in demographic patterns will lead to an exponential increase in the number of elderly individuals who suffer injury from falls, as falls and fall-induced fractures are very common among the elderly.

Hip fractures account for most of the deaths and the costs of fall-induced fractures. Worldwide, there are around 4,000,000 hip fracture cases every year, and the annual mortality rate is 30.8%. In Hong Kong, there are 4,000 cases per year [2]. This leads to HK$150 million in medical and rehabilitation expenditure. There are many commercially available hip protectors that are composed of a pair of hard pads that are worn with a tight undergarment. Some of them are proven to have force attenuation abilities as high as 95% [3]. However, it is uncomfortable and inconvenient for the elderly to wear such protectors, which leads to a poor compliance rate without achieving the expected prevention of hip fractures. In Hong Kong, hot weather causes a low compliance rate, which averages 40% for the entire year and ranges from 70% in the autumn to 20% in the summer [4]. To build a protective system, the idea of automobile airbag systems is applied. This system has two modules: a sensing module (μIMU) and an inflator that connects to two nylon airbags. When the μIMU detects a fall, it triggers an inflator, which then deploys the airbags before impact to protect the elderly. The gas is supplied from a handy compressed gas cylinder, rather than the combustion of chemicals.

Due to the availability of low-cost, small-sized MEMS sensors, it is possible to build self-contained inertial sensors with an overall system dimension of less than 1 cubic inch and, at the same time, a sensing unit that can track disorientation and other motions in real time. The real-time monitoring of human movement can be employed to facilitate long-term monitoring [5]. Previous studies have also demonstrated the use of similar units to recognize daily life activities to acquire indirect measures of metabolic energy expenditure [6]. Some papers have presented the implementation of a real-time classification system for the types of human movement that are associated with motion sensing data [7]. However, the sampling rate is too low, and the system is only suitable for normal life recording and analysis. Few μIMU systems are designed for real-time interaction with human and mechanism systems for further action.

Our group has developed a Micro Input Device System (MIDS) based on MEMS sensors as a novel multi-functional interface input system that could potentially replace the mouse, pen, and keyboard as input devices to a computer [8, 9]. We have also developed a μIMU that measures three-dimensional angular rates and accelerations based on MEMS sensors. We integrated a microcontroller and a Bluetooth module on the μIMU, and the overall size of the unit is less than 66 mm x 20 mm x 20 mm. We developed the module as a ubiquitous wireless digital writing instrument that interacts with humans and computers [10]. A human airbag system is another application. Along with the μIMU, it combines an SVM (Support Vector Machine) filter [11], an embedded DSP, and a mechanical system for airbag deployment.

This paper describes the development of the human airbag system. First, a mechanical airbag deployment system is finalized. The weight of the prototype is 253.5 g, including a 42.5 g compressed $CO_2$ cylinder. The length, width, and thickness of the inflator are 190 mm, 57 mm, and 30 mm, respectively. The inflator response time is 0.133 seconds after receiving a signal from the sensor, and the total inflation time for a 2.06 L custom-made nylon airbag is 0.6 seconds. Second, with the analysis of high-speed camera data, a gate filter is generated and fit to the μIMU, and an independent airbag release experiment showed that the μIMU cooperates well with the deployment system for hip protection. The paper is organized as follows. In Section 2, the airbag system is introduced, including μIMU hardware, the SVM process, and the design of the deployment system. Section 3 focuses on an independent demonstration based on high-speed camera analysis. Section 4 introduces real-time realization with the new SVM filter. The embedded DSP system shows the real-time classification and proves the feasibility of our system. Finally, our conclusions are presented in Section 4.

## II HUMAN AIRBAG SYSTEM FOR FALL PROTECTION

As mentioned above, hip fractures account for most of the costs of falls and fall-induced fractures, especially for elderly people. We propose the development of intelligent and personalized wearable airbags to reduce the impact force of falls for the elderly. Figure 1 illustrates the basic concept of the intelligent human airbag system. Initially, the airbag is compressed in a belt. When an elderly person loses his or her balance, the MEMS micro sensors in the belt detect his or her disorientation and trigger the inflation of the airbag on the correct side in a few milliseconds before the person falls to the ground. There are two main parts to this project. One is the electronic part that works with an algorithm to judge a fall and send a trigger signal to the airbag inflator. The other is the mechanical part, which includes the inflator structure for compression, airbag deployment control, and airbag design.
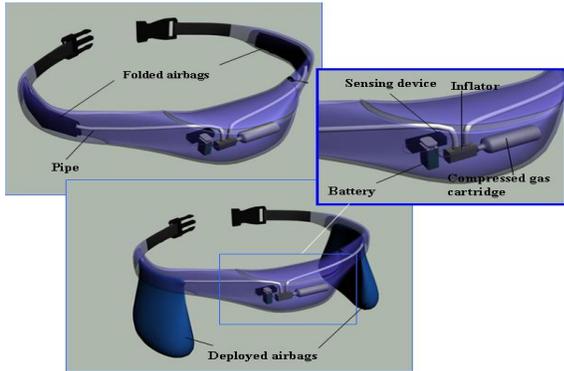


Figure 1. Conceptual illustration of the "intelligent" human airbag system.

### A. µIMU and SVM algorithm

#### a) µIMU design

MEMS sensors play a major role in the µIMU due to their low cost and miniature size. For our experiments, we use ADXL203 (**AD Inc.**) sensors as accelerometers [12] and **muRata** ENC-03 angular rate gyros, respectively. These are low-cost and relatively high-performance sensors with analog signal output. The output signals of the accelerometers ($a_x$, $a_y$, $a_z$) and the angular rate gyros ($\omega_x$, $\omega_y$, $\omega_z$) are measured directly with an A/D converter inside the microcontroller. We use an ATMEL ATmega32 microcontroller in the design. This microcontroller has 32 Kbyte flash, 2 Kbyte of SRAM, 8 channels of 10-bit ADC, and a USART (Universal Synchronous and Asynchronous serial Receiver and Transmitter) port. The digital sample rate of the microcontroller is 200 Hz, which ensures rapid reaction to human motion. We adopt a TDK Systems blu2i Module in our system to transfer data to a host system. This Bluetooth module provides easy integration to various host systems. The module is directly connected to the microcontroller via a USART port. The module is very small in size (66 mm x 20 mm x 20 mm) and can easily communicate with the microcontroller.

The accelerometers and the gyros act as a micro inertial measurement unit (µIMU) of the motion sensing system. These µIMU sensors and the Bluetooth module are housed on a small PCB, as shown in Fig. 2. Two Li batteries of 3.6 V can power the unit for ~3 hours. Thus, the µIMU can realize two functions: 1) data collection and transmission to the computer wirelessly, which can be analyzed or trained using an SVM. Later, the data can be transmitted to DSP chips for real-time analyses, and 2) a gate recognition algorithm can be downloaded to discriminate a falling motion and trigger the airbag for inflation.
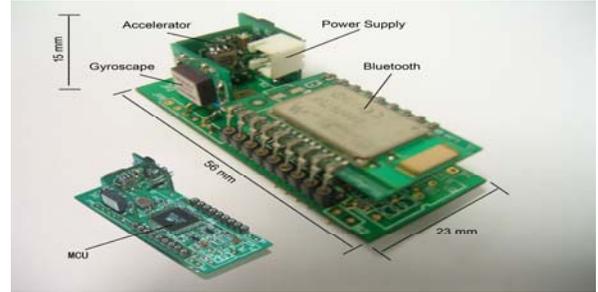


Figure 2. Photograph of a 3-D motion sensing system consisting of 3 gyros and 3 accelerometers sensors.

#### b) SVM training process

Although a simple angular rate threshold can describe that a fall is happening, false inflations can occur during normal physical activity. We must make the trigger device reliable, which means the sensing unit must trigger the deployment system when a fall occurs, and, at the same time, a wrong signal should not be generated to avoid unnecessary panic, especially for the elderly. The SVM, a kind of neural network algorithm, is selected because it is a good binary classifier with relative fewer samples. An SVM-based scheme using a host computer was tested to distinguish between normal and falling motions. We are currently testing an embedded SVM filter in DSP chips and have had relatively good simulation results in computational time consumption.

As shown in Figure 3, the MCU first converts the sensor outputs to digital signals and then transmits the packed data signal sequentially via a Bluetooth module to a computer. Hundreds of recordings, including lateral falls, walking, running, sitting, walking up and down stairs, and stepping in elevators, were made to form a database for SVM training. After training, we selected the best features to form a classifier for falling-motion recognition.

Our goal is to recognize a falling-down motion in real time to control a hip-protection airbag. We address this problem as binary pattern recognition with SVM, as follows.

(1) Set up a motion database of "falling-down" and "non-falling-down" examples using the uIMU.

(2) Use a supervised PCA (Principle Component Analysis) to generate and select characteristic features.

(3) Implement SVM training (Support Vector Machine) to produce a classifier.

The basic idea of SVM is to map the data $X$ into a high-dimensional feature space $f$ via a nonlinear mapping $\Phi$, and to do linear regression in this space [11]:

$$f(\bar{x}) = (\omega \cdot \Phi(\bar{x})) + b \quad (\Phi : R^N \to F, \omega \in F) \quad (1)$$

where $b$ is a threshold. Thus, linear regression in a high dimensional (feature) space corresponds to nonlinear regression in the low dimensional input space $R^N$. Since $\Phi$ is fixed, we determine $\omega$ from the data by minimizing the sum of the empirical risk $R_{emp}[f]$ and a complexity term $\|\omega\|^2$, which enforces flatness in feature space:

$$R_{reg}[f] = R_{emp}[f] + \lambda \|\omega\|^2 = \sum_{i=1}^{l} C(f(\bar{x}_i) - y_i) + \lambda \|\omega\|^2 \quad (2)$$

where $l$ denotes the sample size $(\overline{x}_1,\ldots,\overline{x}_l)$, $C(.)$ is a loss function and $\lambda$ is a regularization constant. Taking (1) and (2) into account, we are able to rewrite the whole problem in terms of dot products in the low dimensional input space

$$f(\overline{x}) = \sum_{i=1}^{l} (\alpha_i - \alpha_i^*)(\Phi(\overline{x}_i) \cdot \Phi(\overline{x})) + b$$
$$= \sum_{i=1}^{l} (\alpha_i - \alpha_i^*)K(\overline{x}_i,\overline{x}) + b \quad (3)$$

where $\alpha_i$, $\alpha_i^*$ are Lagrangian multipliers, and $\overline{x}_i$ are support vectors.
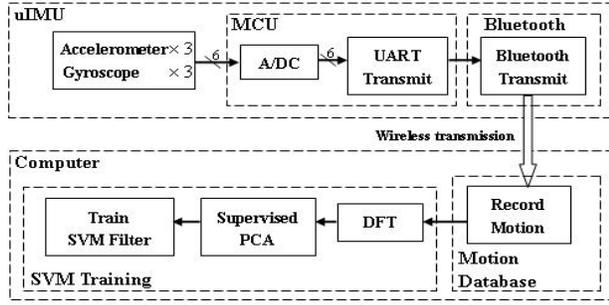


Figure 3. Schematic chart of SVM training.

## B. Airbag release system

The mechanical release mechanism includes a cross-shaped punch mounted on a launcher that consists of a spring and a locking switch. The spring is compressed by screwing. When the locking switch is pressed by an actuator, the compressed spring extends, and the punch accelerates toward the pressurized cylinder. The compressed $CO_2$ is released from the gap between the punch and the cylinder cap. Finally, the gas is transmitted along a 16-cm-long pipe to inflate the airbag.

The actuator used is a 16 g commercially available servo BMS-380MAX that is 26 x 13 x 26 mm in size, with a speed of 0.15 sec/60 deg at 4.8 V. It requires only 5 V and less than 0.6 A. The maximum torque is 4.1 kg/cm at 4.8 V (Fig. 4).
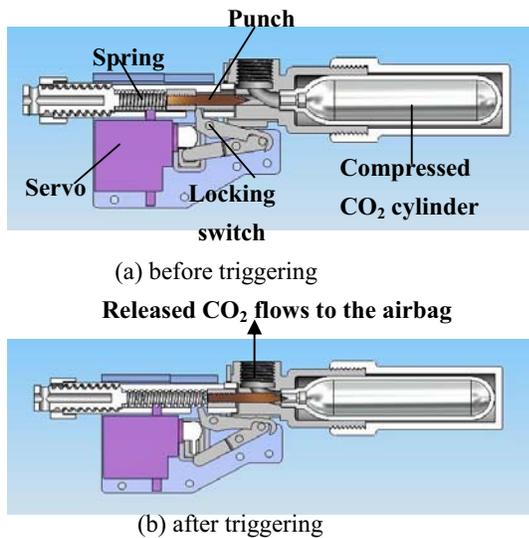


(a) before triggering



(b) after triggering

Figure 4. The cross-sectional view of the inflator.

We have also engineered the airbag inflation process to ensure that the airbags could be inflated within 0.333 sec, i.e., the entire fall-sensing, mechanical triggering, and airbag inflation process must be completed within ~0.9 sec in order for the system to protect a falling human. The classical compressible-fluid mass flow rate equations are used to estimate flow parameters through an orifice:

$$W_{12} = \frac{A_{12}P_1}{\sqrt{T_1}} \left\{ \frac{2\gamma}{R(\gamma-1)} \left[ \left(\frac{P_2}{P_1}\right)^{2/\gamma} - \left(\frac{P_2}{P_1}\right)^{\gamma+1/\gamma} \right] \right\}^{1/2} \quad (\frac{P_2}{P_1} > 0.528)$$

$$W_{12} = \frac{A_{12}P_1}{\sqrt{T_1}} \left\{ \frac{\gamma}{R} \left[ \left(\frac{2}{\gamma+1}\right)^{(\gamma+1)/(\gamma-1)} \right] \right\}^{1/2} \quad (\frac{P_2}{P_1} \le 0.528)$$

(4)

where $W$ is mass flow rate (Kg/s), $A_{12}$: the area of the inlet orifice of airbag (in $m^2$), $\gamma$ is the specific heat ratio ($\gamma = 1.4$ for air, 1.3 for $CO_2$), $R$ is the gas constant ($R = 287$ J/Kg K for air, 188.9 J/Kg K for $CO_2$). In addition, equations below describe instantaneous pressure in the compressed gas cylinder under subsonic flow and sonic flow respectively:

$$\frac{dP_1}{P_1} = -N_{12} d\left(\frac{KR\sqrt{T_0}A_{12}}{V_1}t\right) = -N_{12}d\tau$$
$$P_1 = P_0 e^{-\tau}$$

(5)

where $\tau = \frac{KR\sqrt{T_0}A_{12}}{V_1}t$, $N_{12}$ is the ratio of mass flow rate to choked mass flow rate. For subsonic flow, $N_{12}$ will vary with the pressure ratio and the differential equation can be solved by Matlab Simulink. Figure 5 shows pressures and mass flow rate comparison between simulation and experimental result (using outlet orifice of 15.21 $mm^2$ at initial pressure of 550 kPa). It is clear that the equations above are sufficient in modeling the gas flow parameters during the airbag inflation process.
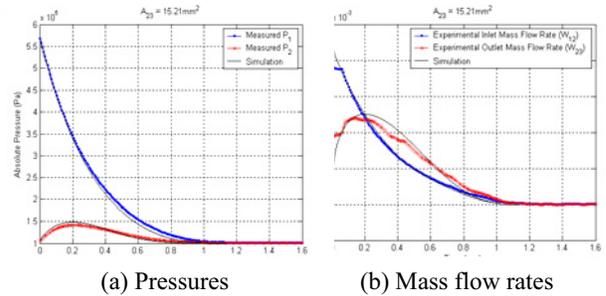


(a) Pressures     (b) Mass flow rates

Figure 5. Comparison of experimental and simulation results of mobile airbag inflation.

## III  INDEPENDENT AIRBAG SYSTEM

### A. High-speed camera analyses

To analyze the µIMU signal output, a high-speed camera was used to record the falling motion while the µIMU was in operation. The camera model was a PCO 1200 hs High-Speed Cam with a maximum resolution of 1280 x 1025 pixels. The film rate used was 200 Hz. The camera was placed 5 m away and orthogonal to the falling direction. By measuring the inclined angle of the trunk ($\theta_i$) in the films between the known time intervals, the change of the inclined angle with respect to time can be obtained. The angle-time relationship can be fitted with a cubic curve. The instantaneous angular velocity of the hip can be measured by differentiating this cubic curve. Moreover, when compared to one of the gyro outputs (the rotational velocity of the trunk) of the µIMU, the signal corresponding to impact can be justified. In Figure 6, the inclined angle of the trunk ($\theta_i$) is

measured from the film output of the high-speed camera. $\theta_i$ is determined from the feature with the horizontal line in the film.
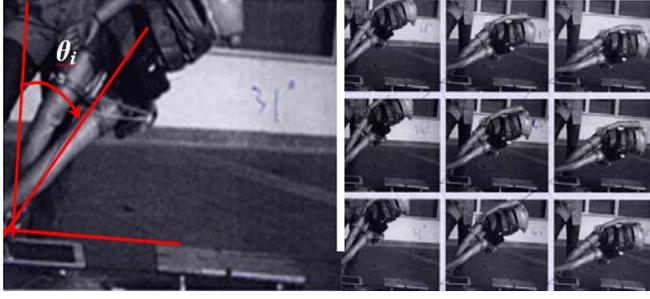


Figure 6. Fall analysis with high-speed camera.

Figure 7 shows that the angle-time relationship can be fitted with a cubic curve. The instantaneous angular velocity of the hip can be measured by differentiating this cubic curve.
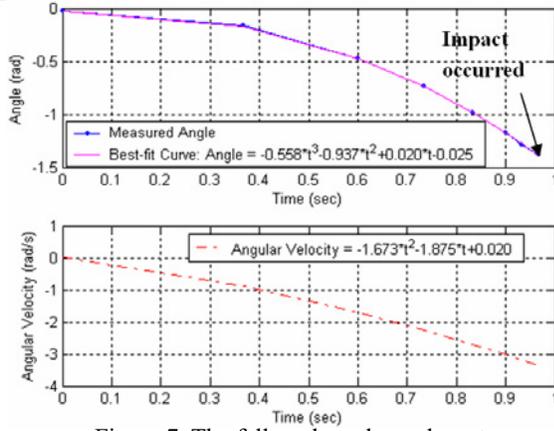


Figure 7. The fall angle and angular rate.

As shown in Figure 8, when we compared the high-speed camera result with one of the gyro outputs (the rotational velocity of the trunk) of the µIMU, the signal corresponding to impact can be justified. The gyro output is very similar to the image analysis. This also helps us to determine when we should open the airbag.
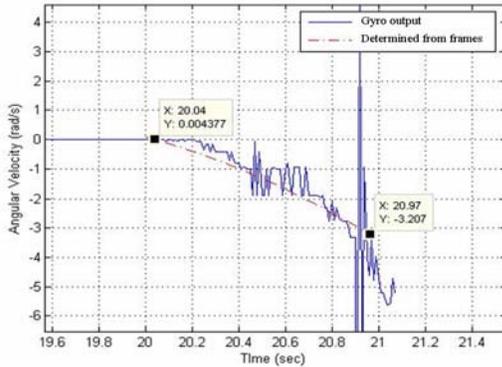


Figure 8. Comparison of high-speed camera result and the gyro sensor output.

**B. Airbag system demo**

With the results of the high-speed camera and the inflator, we can set up a demo to show to the feasibility of the airbag system. We connected the air cartridge and the inflator, and the inflator was connected to the µIMU, which will trigger it. A certain gyro sensor value was set as the threshold of a dangerous fall. As we assumed that after a 30-degree angle, a person cannot maintain his or her balance any longer, we traced the value of angular velocity from the high-speed camera results and put it to the gyro sensor. The digital number of the gyro sensor is 279, which means that when the sensor output is lower than 279, the µIMU will trigger the airbag for an action.

Figure 9 shows the results of airbag deployment. When a person is falling, and the angular velocity is larger than a given value, the sensor module will trigger the $CO_2$ cylinder to release air for airbag inflation. We can clearly see that the airbag is inflated before the person falls to the ground, which provides hip protection. This experiment proves that the airbag system is feasible.
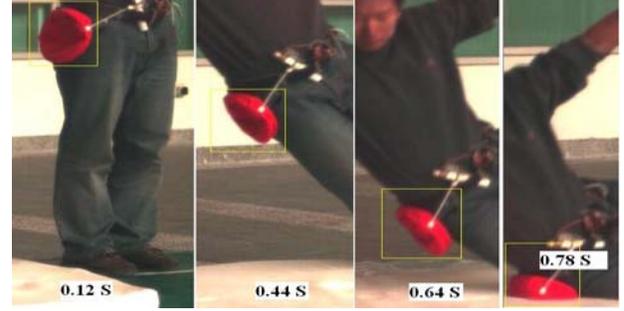


Figure 9. Independent demonstration with µIMU and deployment system.

## IV  REAL TIME APPLICATION WITH DSP

We recorded 200 experimental results, half of which were "falling-down" data and half "non-falling-down" data. Each result consisted of six arrays measured by the six sensors.

We performed data pre-processing to filter noise and reduce the dimension. For each experimental result, we performed a DFT of the six arrays, respectively. We kept the first 10 coefficients of each DFT result. After 200 DFTs, we obtained a matrix of 200 rows and 60 columns, each row representing an experiment. Each has 6*10 numbers in the sequence *Gx, Gy, Gz, Ax, Ay, Az*.

We found that compressing the training data to three dimensions using PCA was sufficient to obtain good classification results. We randomly chose half of the data for SVM training, and the other half was used for testing. On the unseen testing data, good results were obtained, and the resulting system could classify the test vectors into "falling-down" and "non-falling-down" states without error. Equation 6 is the computation required for the SVM classifier:

$$f(x_1, x_2, x_3) = c_0 + c_1 \cdot x_1 + c_2 \cdot x_2 + c_3 \cdot x_3 + c_4 \cdot x_1^2 \qquad (6)$$
$$+ c_5 \cdot x_1 \cdot x_2 + c_6 \cdot x_1 \cdot x_3 + c_7 \cdot x_2^2 + c_8 \cdot x_2 \cdot x_3 + c_9 \cdot x_3^2$$

The corresponding coefficients are shown in Table 1. Although the training process is computationally expensive, the computational requirements of the classifier after training are very small.

Table 1.  The coefficients of the SVM classifier.

| | | | |
|---|---|---|---|
| $c_0$ | -4.114032908 | $c_5$ | -0.000013017 |
| $c_1$ | 0.029363568 | $c_6$ | 0.000056986 |
| $c_2$ | 0.009281220 | $c_7$ | 0.000004560 |
| $c_3$ | 0.004760046 | $c_8$ | -0.000013625 |
| $c_4$ | -0.000004642 | $c_9$ | 0.000052657 |

## A. Improvement of SVM filter: Window processing

For a real-time system, our goal is to realize an algorithm that can recognize a fall before it is completed. The system must recognize a dangerous action in a very short time to ensure that there is enough time for airbag inflation. At the same time, the system should not be falsely triggered when a person is going through normal motions.

We suggest a slide window processing algorithm, i.e., defining a certain width of 'window' for processing. We cut a selected 'window-width' for FFT and SVM filter judging, and, at the same time, the window is pushed forward; hence, the data in the window could be judged every 1/200 seconds.

Figure 10 shows the process of 'window cutting'. We first define the width of the window, then push it forward. At every cut, the six-dimensional sensor information, including accelerations and angular rates, is analyzed.
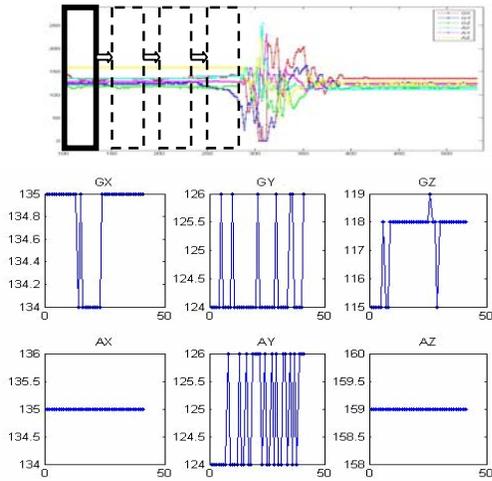


Figure 10. Window cutting processing.

Window widths of 40, 50, 60, and 70 (200 Hz) for all 100 falling experiments and 1,000 other motions, including running and walking, etc., were used for SVM training. The result is that the falling motion and the other motions can be totally separated using all these window widths. Figure 11 shows the results in a Matlab figure, in which the blue points represent the fall data, and the red points represent the other motions.
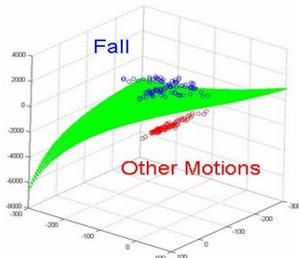


Figure 11. Falling and other motions can be classified.

## B. Improvement of SVM filter: Lowering the sampling rate

As defined above, the sampling rate of our μIMU is 200 Hz. For the window process algorithm, every 0.005 seconds, a new array of six channels of data will renew the FFT results of the 60*1 polynomial. In this very short time, the system must recognize whether the motion is dangerous, which means the FFT and the SVM filter computations should be completed in 0.005 seconds. Assuming our DSP has a 300 MHz clock rate, then the whole filter process must be done in 1.5 M

instructions. Figure 12 shows the computation requirements of this filter process. In our most updated system, 200 Hz ADC data is transmitted, but the data is sampled and trained every 10 milliseconds. And, with the SVM training process, a filter for fall detection is generated. The results show that we can classify falling and other motions clearly. Therefore, this new filter can be loaded to a DSP, and the calculation time can be prolonged to 10 milliseconds.
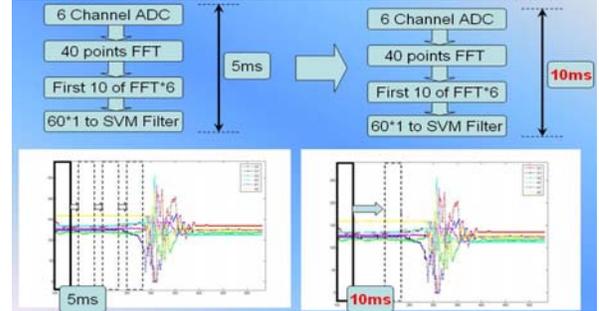


Figure 12. The filter computations can be performed in 1/100 second.

## C. DSP implementation

As described above, for a real product, we must integrate all of the algorithms into one chip. For a high-speed DSP, there is no analog-to-digital port, so we use the existing sensor data for testing. This means we transfer all of the data into the DSP first, let the algorithm read the data with the fixed slide window, and then judge each window for danger. Figure 13 shows the algorithm flow of the system.
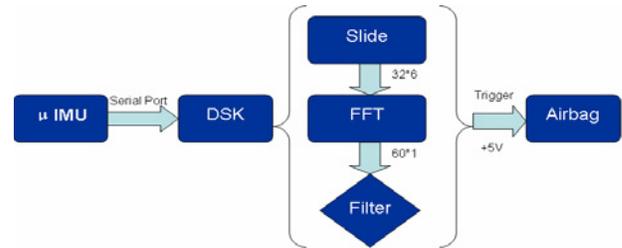


Figure 13. Real-time product structure.

The TMS320 6713 DSP chip is used for our system. The C6713 device is based on the high-performance, advanced very-long-instruction-word (VLIW) architecture developed by Texas Instruments (TI), making it an excellent choice for multichannel and multifunction applications. The key issue for selecting a DSP is operation speed, which makes the C6713 device a suitable choice [13].

### a) Computation time consumption for DSP

FFT is widely used for frequency domain processing and spectrum analysis. It is a computationally efficient discrete Fourier transform (DFT), which is defined as

$$X(k) = \sum_{N=0}^{N-1} X_n W_N^{kn}, \quad k = 0,..., N-1, \tag{7}$$

where the twiddle factor is defined as

$$W_N^{kn} = e^{-2j\,\pi n k/N}. \tag{8}$$

So, for each value of $k$, the direct computation of $X(k)$ involves complex multiplication and complex additions. Consequently, to compute all values of DFT requires $N^2$ complex multiplications and $N^2-N$ complex additions. The main duty of the FFT algorithms is complexity reduction, by way of decomposing the DFTs into smaller DFTs in a

recursive manner. The most popular decomposition method is radix-2 decomposition. Here, the entire DFT sequence is decomposed into two smaller DFTs, which are further divided into two smaller DFTs, and so on. The recursion ends when the smallest DFT is reached: a two-point-DFT called "butterfly." This method significantly reduces the complexity of the DFT. The reduced complexity of the radix-2 FFT algorithms is $(N/2)*log_2(N)$ complex multiplications and $(N)*log_2(N)$ complex additions [13].

An experiment shows that FFT simulation based on the radix-2 FFT algorithm (367,111 cycles for a DSP of 300 MHz) will cost ~0.001 seconds, which is insignificant compared to the time-cost for the mechanical systems.

### b) SVM filter consumption

As mentioned above, we need to generate $x_1$, $x_2$, $x_3$ before the SVM filter, as shown in Equation (1). Originally, we had the first 10-order FFTs of the six ADC channels; therefore, a 60*1 polynomial is generated. In the SVM training process, we have one parameter matrix (60*3). This 60*1 polynomial multiplies with the parameter matrix, resulting in a 3*1 ($x_1$, $x_2$, $x_3$) polynomial that is ready for the final filter:

$$f(x_1,x_2,x_3) = c_0 + c_1 \cdot x_1 + c_2 \cdot x_2 + c_3 \cdot x_3 + c_4 \cdot x_1^2$$
$$+ c_5 \cdot x_1 \cdot x_2 + c_6 \cdot x_1 \cdot x_3 + c_7 \cdot x_2^2 + c_8 \cdot x_2 \cdot x_3 + c_9 \cdot x_3^2 \quad (6)$$

For the matrix calculation, 180 multiplications and 180 additions are required. For the filtering algorithm, 15 multiplications and nine additions are needed.

An experiment shows the simulation results of the SVM filter, which includes the 60*1 FFT result, and the cycles are about 66,910. A DSP of 300 MHz costs 0.00002 seconds.

In the simulation result, the entire consumption of the DSP is 434,021 cycles, whereas, in real-time computation, our new filter gives us 3 M cycles for calculation, which is enough if we take the simulation result.

### c) Demonstration for DSP real-time classification

Figure 14 shows a demo of the DSP system in recognizing a fall motion. An integrated algorithm is embedded in the DSP. The algorithm performs FFT and SVM, which discriminates normal motions (walking, going up stairs, sitting, standing) from falls. As the photos show, the airbag is triggered only when a fall occurs. This demo proves the feasibility of the real-time DSP application and the entire airbag system.
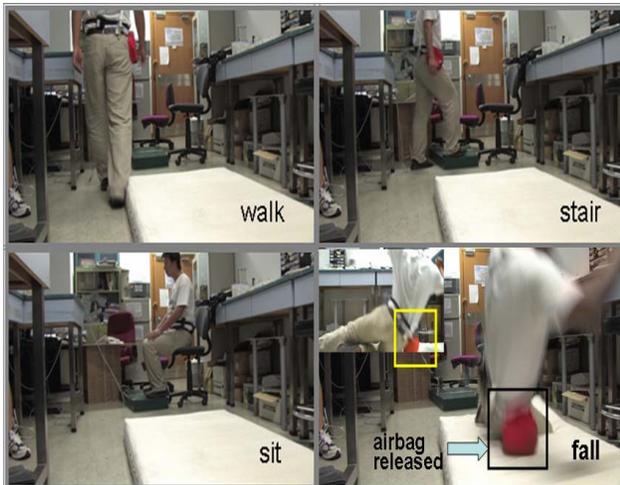


Figure 14. Demonstration of fall protection in real-time.

## IV CONCLUSION

This paper presents a novel MEMS-based human airbag system that is under development. A Micro Initial Measurement Unit (μIMU) is used for the detection of complex human motions and the recognition of a falling-down motion, which can then be used to trigger the release of airbags. An air release system is also designed. Combined with our μIMU, we set up an independent demo to demonstrate that the airbag system is feasible. We also use SVM as a pattern recognition method for training after PCA for the DFT data. We have shown that selected eigenvector sets can classify 200 experimental data sets to generate the eigenvectors into "non-falling-down" or "falling-down" categories. With the improvement of our SVM filter, the algorithms can easily be embedded into a real-time DSP. The experiments show that the embedded algorithms can classify fall and non-fall in real time and the airbag can be deployed when fall occurs.

## REFERENCES

[1] Myo Naing Nyan, Francis Eng Hock Tay, Teck Hong Koh, Yih Yiow Sitoh and Kwong Luck Tan, "Location and sensitivity comparison of MEMS accelerometers in signal identification for ambulatory monitoring", Electronic Components and Technology, June, 2004. Vol. 1, 1-4, Page(s):956-960.

[2] Chan J., Lam P.S., Sze P.C. and Leung K.S., "A study of the epidemiology of falls in Hong Kong", Symposium on Preventing Falls and Fractures in Older Persons, Yokohama, Japan, July, 2004.

[3] Kannus P., Pakkari J., and Poutala J., "Comparison of force attenuation properties of four different hip protectors under simulated falling conditions in the elderly: An in vitro biomechanical study", Bone, 1999. Vol. 25, Page(s):229-235.

[4] Sze P.C., "Mechanical and compliance study of a modified hip protector for old age home residents in Hong Kong", MPhil Thesis, The Chinese University of Hong Kong, 2006.

[5] Nakahara A.K., Sabelman E.E. and Jaffe D.L., "Development of a second generation wearable accelerometric motion analysis system", BMES/EMBS Conference, Proceedings of the First Joint, Oct. 1999. Vol. 1, 13-16, Page(s):630.

[6] C.V. Bouten, K. T. Koekkoek, M.Verduin, R. Kodde and J. D. Janssen, "A triaxial accelerometer and portable data processing unit for the assessment of daily physical activity", IEEE Trans. on Biomedical Engineering, Mar. 1997. Vol. 44, no. 3, Page(s):136-147.

[7] Karantonis D.M., Narayanan M.R., Mathie M., Lovell N.H. and Celler B.G., "Implementation of a real-time human movement classifier using a triaxial accelerometer for ambulatory monitoring", IEEE Trans. on Information Technology in Biomedicine, Jan. 2006. Vol. 10, Issue 1, Page(s):156-167.

[8] A.H.F. Lam, Wen J. Li, Yunhui Liu and Ning Xi, "MIDS: micro input devices system using MEMS sensors", IEEE/RSJ International Conference on Intelligent Robots and System, Oct. 2002. Vol. 2 , no. 30, Page(s):1184-1189.

[9] A.H.F. Lam, R.H.W. Lam, W.J. Li, M.Y.Y. Leung and Yunhui Liu, "Motion sensing for robot hands using MIDS", ICRA '03. IEEE International Conference on Robotics and Automation, Sept. 2003. Vol. 3 ,14-19, Page(s):3181-3186.

[10] Guanglie Zhang, Guangyi Shi, Yilun Luo, H. Wong, Wen J. Li, P.H.W. Leong and Ming Yiu Wong, "Towards an ubiquitous wireless digital writing instrument using MEMS motion sensing technology", IEEE/ASME International Conference on Advanced Intelligent Mechatronics 2005, Page(s):795-800.

[11] Yilun Luo, Guangyi Shi, Josh Lam, Guanglie Zhang, Wen J. Li, Philip H. W. Leong, Pauline P.Y. Lui and Kwok-Sui Leung, "Towards a Human Airbag System Using μIMU with SVM Training for Falling-Motion Recognition", IEEE Int. Conf. on Robotics and Biomimetics (IEEE ROBIO) 2005, Hong Kong, June 29-July 03, 2005.

[12] Analog Devices Inc. Precision ±1.7 g Single/Dual Axis Accelerometer ADXL203 Datasheet, 2004.

[13] www.ti.com.